ELSEVIER

Polymer 42 (2001) 6877–6890

polymer

www.elsevier.nl/locate/polymer

Miscibility of linear and branched polyethylene blends by thermal fractionation: use of the successive self-nucleation and annealing (SSA) technique

M.L. Arnal, J.J. Sánchez, A.J. Müller*

Departamento de Ciencia de los Materiales, Grupo de Polímeros USB, Universidad Simón Bolívar, Apartado 89000, Caracas 1080-A, Venezuela

Received 21 November 2000; received in revised form 13 February 2001; accepted 16 February 2001

Abstract

In the present work, the recently developed thermal fractionation technique successive self-nucleation and annealing (SSA) was applied to blends of branched and linear polyethylenes (PEs), as a method to evaluate the phenomena of miscibility and segregation in PE blends. The melting behavior of the systems, after a controlled cooling and after the application of SSA was compared.

The DSC scans corresponding to cooling of blend samples from the melt or subsequent heating displayed an overlap of the exotherms and endotherms, respectively, of the blend components that could lead to interpretations of partial miscibility. These effects were interpreted as arising from: a nucleation effect of the crystals formed by the more linear PE on the crystals of branched PE, a dilution effect of the molten branched chains on the crystals formed by the more linear PE and finally possible partial miscibility effects. However, after SSA, even when the nucleation and dilution effects are still present for some of the fractions produced, the thermal fractionation procedure helps to distinguish them from co-crystallization effects. This is mainly achieved by observing how the number of thermal fractions generated by SSA in the blends varies with composition and by comparing the relative amounts of the thermal fractions produced by SSA.

The results indicate that only those PE fractions that are similar in chemical structure, as regards to content and distribution of short chain branches, are probably miscible in the melt and can oppose molecular segregation during SSA and therefore produce stable co-crystals in the solid state. The application of SSA to the study of PE blends can be a quick and convenient tool for making comparisons and ascertain miscibility of different types of PE blends.

Keywords: Successive self-nucleation and annealing; DSC; Polyethylene blends

1. Introduction

It has been recognized that the crystalline morphology of blends of linear and branched polyethylenes (PEs) depends on the following factors: cooling conditions, the crystallization properties of each component which are related to its molecular structure (molecular weight, branching), the composition of the mixtures and melt homogeneity. There exists an interest in establishing how these factors determine the occurrence of co-crystallization (miscibility in the solid phase usually arising as a consequence of quenching a miscible melt) or molecular segregation of the components during cooling [1–13].

A variety of studies report that upon evaluating blends of linear low-density polyethylene (LLDPE) and high-density polyethylene (HDPE) by differential scanning calorimetry (DSC), if their thermal behavior shows a unique crystallization signal and melting at temperatures between those of pure components, this may be taken as an evidence of miscibility in the system [2,4,6–9]. However, the dependency of the position of these peaks with composition, is variable, and a trend which complies with a simple law of mixing has been reported [4,9] as well as strong positive deviations from it for compositions of 70–80% LLDPE [2,6–9] or complex dependencies [8]. However, Datta and Birley [2] indicate that a single thermal transition cannot, by itself, be considered as definitive evidence of co-crystallization, given that phenomena of coincidental crystallization or nucleating effects in the system, may be present. Norton and Keller [3] and Barham et al. [5] report partial miscibility in LLDPE or low-density polyethylene (LDPE) mixtures with HDPE, establishing that the crystalline phases detected are only possible as a consequence of the existence of a liquid–liquid phase separation in the melt. This statement has been validated upon analyzing the melting of PE mixtures by small angle neutron scattering (SANS) [12]. In a counter-view, Tashiro [10] and Wignall et al. [11]

---

* Corresponding author.
E-mail address: amuller@usb.ve (A.J. Müller).

0032-3861/01/$ - see front matter
PII: S0032-3861(01)00177-X

obtained SANS evidences of a one phase melt of linear and branched PE. Upon cooling this homogeneous melt, results were obtained that indicated segregation during crystallization. In the case of ultra low-density polyethylene (ULDPE) and HDPE, Kim et al. [13] have reported that the mixture is generally immiscible both in the melt and the solid state, even though miscibility can be observed in compositions that are rich in HDPE.

On the other hand, the copolymerization of ethylene with α-olefins, using new developments in catalytic systems and improvements in the processes of synthesis, allows density grades between 0.875 and 0.910 g/cm^3 to be obtained. These grades are lower than those prepared in the past by conventional LLDPE obtained with conventional Ziegler–Natta catalysis [14–16]. These new resins have been designated as very low-density polyethylene (VLDPE) and ULDPE. In ethylene and α-olefin copolymers, the study of the architecture of the molecular chain is an essential parameter in understanding the properties of these resins, particularly in the solid state. It is important to know the type of α-olefin used, its content in the copolymer and the specific distribution of the α-olefin or short branches in the material [16–19].

The characterization of the branching distribution, in ethylene and α-olefin copolymers, has typically been done by the temperature rising elution fractionation technique (TREF) [19]. Recently, Monrabal [20] has designed an equipment that permits the measurement, in solution, of the concentration of the copolymer molecules, as a function of the temperature of crystallization. This technique which has been called crystallization analysis fractionation (CRYSTAF) allows data somewhat equivalent to TREF to be obtained. Additionally, several methods of thermal fractionation have been designed using DSC. Usually, a process of step crystallization (SC) from the melt is applied to the sample. This process has been inspired by the cooling procedure that takes place in the TREF, although generally no solvent is involved. The results, obtained in a shorter time, give preliminary qualitative information of the distribution of the α-olefin in the copolymer [21–38].

Our group has recently developed a thermal fractionation technique designed to produce better fractionation in PE than SC by DSC, using shorter times, since the method involves a more complex thermal treatment that allows better resolution [39–42]. This method is similar to that published in 1964 by Gray and Casey [43]. The successive self-nucleation and annealing (SSA) technique is based on the sequential application of self-nucleation and annealing steps to a polymer sample, where each cycle is similar to those designed by Fillon et al. [44], for the evaluation of the self-nucleation process in PP. After thermal conditioning, a final DSC heating run reveals the distribution of melting points induced by the SSA treatment, as a result of the heterogeneous nature of the chain structure of the polymer under analysis. The nature of the polymer chain must be heterogeneous in order to have a wide distribution of crystallizable chain segments. We have applied SSA to the characterization of different PE grades [39], functionalized LLDPE and ULDPE [40,42,45], cross-linked PE [42], and to confined chains of crystallizable polymers within microphase separated block copolymers [42,46]. More recently, SSA has proven useful to follow hydrolytic degradation in poly(*p*-dioxanone), a biodegradable polymer [47].

With reference to the study of blends of PE, both TREF [48,49] and thermal fractionation by SC [23,36,50] have been used as tools for evaluating the miscibility of components. Shanks and Amarasinghe [50] reported recently the use of SC methods to study the miscibility of LLDPE and VLDPE blends. These authors interpreted as evidence of co-crystallization the observation of differences in the number of thermal fractions generated by SC and that expected on the basis of the fractionation of the neat components. In this work, the use of the SSA technique is presented as an alternative to evaluate the miscibility of the LLDPE/HDPE and ULDPE/HDPE blends. The present work extends our previous short communication on this subject [41].

2. Experimental

2.1. Materials and blend preparation

The grades of PEs used in this study were:

(a) Two HDPEs manufactured in Venezuela by Poliolefinas Internacionales, POLINTER, both obtained by slurry processes: an injection grade, Altaven 2208J, which is a homopolymer with unimodal molecular weight distribution (HDPE1), and a blown film grade, Altaven 7000F, an ethylene/1-butene copolymer with bimodal molecular weight distribution (HDPE2).
(b) A blown film grade LLDPE, Sclair 11U4, an ethylene/1-butene copolymer produced by DuPont Canada, synthesized by a solution process.
(c) An experimental grade ULDPE produced by Enichem Polimeri (Italy), NULDI, an ethylene/propene/1-butene terpolymer produced by a modified high pressure process using supported Ziegler–Natta (Z–N) catalytic system.

Some basic molecular and thermal characteristics of these PEs are presented in Tables 1 and 2. The blends were prepared in a wide composition range using a Haake Rheocord EU10, co-rotating, double screw extruder. The extrusion conditions were 40 rpm and a temperature of 210°C at the die. They were later compression molded at 170°C into 0.5 mm thick sheets. The blends systems prepared were: LLDPE/HDPE1, LLDPE/HDPE2 and ULDPE/HDPE2.

2.2. Evaluation of basic thermal behavior

A Perkin–Elmer DSC-7 calorimeter was used to record cooling runs down to 25°C, after complete melting for 3 min

Table 1
Physical and molecular weight data of neat polymers

Resins	Type	Density (g/cm^3)	MFI[a] (dg/min)	$\bar{M}_n/\bar{M}_w$	SBC[b] (–CH$_3$/1000C)
HDPE1	Homopolymer	0.968[c]	5.80	28,500/168,000	–
HDPE2	Ethylene/1-butene copolymer	0.956[c]	0.05	12,500/230,000 bimodal	4.4
LLDPE	Ethylene/1-butene copolymer	0.922[c]	1.40	37,800/159,700	12.7 bimodal
ULDPE	Ethylene/propene/1-butene terpolymer	0.888[d]	2.05	23,000/–	Methyl: 43.5; ethyl: 26.0

[a] ASTM D1238 standard, condition E.
[b] Short chain branching content.
[c] ASTM D1505 standard.
[d] ASTM D792 standard.

Table 2
Thermal properties of PEs measured by DSC

Resins	Crystallization temperature (°C)		Melting temperature (°C)		Observed melting range (°C)	Crystallinity, X_c (%)
	T_c[a]	T_c[b]	T_m[a]	T_m[b]		
HDPE1	115	–	136	–	75–143	80
HDPE2	115	77[b]	131	–	45–136	71
LLDPE	102	63[c]	119	107[b]	35–130[d]	43
ULDPE	78	41[c]	100	67[c]	25–130[d]	20

[a] Evaluated at 10°C/min and crystallinity calculated by DSC heating scans at the same heating rate.
[b] Shoulder.
[c] Peak.

at 170°C, and subsequent heating runs. The heating and cooling rate for these runs was 10°C/min. From the 0.5 mm sheets, small disc samples (with diameters much bigger than their heights) were cut, so that their weight, in all cases, was approximately 10 mg. In this way, the shape, size and weight of all the DSC samples were standardized. The samples were encapsulated in aluminum pans and ultra high purity dry nitrogen was used as an inert atmosphere for all tests. The heat of crystallization (ΔH_c) for 100% crystalline PE was taken as 293 J/g [51].

2.3. SSA technique

The SSA method is performed in a DSC and is described schematically in Fig. 1. The experimental protocol follows:

(a) Erasure of previous thermal history: The sample was first melted at 170°C for 3 min.
(b) Creation of a ‘standard’ thermal history: Immediately following step (a), the sample was cooled at 10°C/min to 25°C, in order to create an initial ‘standard’ thermal history.
(c) Isothermal treatment at T_s (melting and self-nucleation): Subsequently, a heating scan at 10°C/min was performed up to a selected self-seeding and annealing temperature denoted as T_s, where the sample was isothermally kept for 5 min. This first applied T_s was chosen so that the polymer would only self-nucleate (i.e. T_s would be high enough to melt all the crystalline regions except for small crystal fragments and/or nuclei that can later self-seed the polymer during cooling). So, at the end of the first cooling from T_s, the polymer had been self-nucleated as in the regime II, defined by Fillon et al. [44] for self-nucleation.
(d) Cooling down to 25°C (dynamic crystallization from self-nuclei): After the first treatment at T_s described in step (c), the sample is cooled down from T_s at 10°C/min. During cooling, the sample will undergo dynamic crystallization at temperatures higher than in step (b), since the crystals will develop from the self-nuclei produced in step (c).

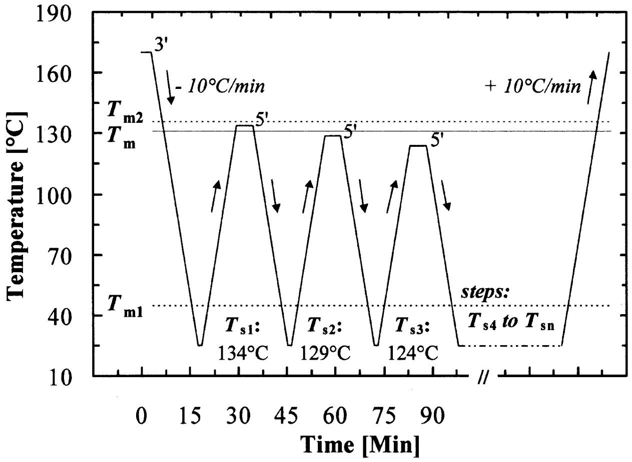

Fig. 1. Basic representation of the experimental protocol of the SSA technique as applied in a DSC.

(e) Isothermal treatment at a lower T_s temperature (partial melting, self-nucleation, annealing of unmelted crystal fraction and isothermal crystallization): After step (d), the sample was heated in the DSC once again at 10°C/min, but this time, up to a T_s which was 5°C lower than the previous T_s. This means that some of the unmelted crystals, at this lower T_s, will anneal during the 5 min at this temperature. Some of the melted species will isothermally crystallize (after being self-nucleated by the unmelted crystal), while the rest of the molten crystallizable chains (or chain segments), will only crystallize during the subsequent cooling from T_s (also from self-nuclei).

(f) The procedure described above for steps (d) and (e) is repeated as indicated in Fig. 1, with T_s being lowered by 5°C intervals with respect to the previous step. The chosen T_s range was 134–109°C for LLDPE/HDPE1 and LLDPE/HDPE2 blends and 134–59°C for ULDPE/HDPE2 blends (see Fig. 1).

(g) Finally, the melting behavior was recorded at 10°C/min when the thermal conditioning was over.

3. Results and discussion

In this section, the thermal behavior observed after cooling from the melt and subsequently heating at 10°C/min for the LLDPE/HDPE1, LLDPE/HDPE2 and ULDPE/HDPE2 systems will be presented. Later, the final heating scans after SSA had been applied will be examined. The interpretation of the results could yield evidences of partial miscibility and/or segregation in the blends and possible differences, after submitting the same blend to a controlled cooling at 10°C/min, or to the SSA treatment.

HDPE1 is a PE that does not have any detectable branching, this is reflected in its high density, high percentage of crystallinity and high melting temperature, see Tables 1 and 2, even though this material shows a polydispersity close to 6. HDPE2 is an ethylene/1-butene copolymer with a lower density and percentage of crystallinity than HDPE1. The LLDPE is also an ethylene/1-butene copolymer with a short chain branching content (SBC) of 12.7 methyl groups per 1000 carbon atoms and exhibits a bimodal melting endotherm (see Fig. 3). Such bimodal melting is composed of a low temperature shoulder and a high temperature peak. The high temperature peak appears to be the overlap of two very close melting peaks or a peak doublet that may be due to reorganization during the scan [52,53].

Finally, ULDPE is an ethylene/1-propene/1-butene copolymer with an elevated quantity of short chain branching, low percentage of crystallinity and with a broad bimodal melting endotherm. We have previously reported the qualitative characterization of the branching distribution of materials that are very similar to HDPE2, LLDPE and ULDPE using the SSA technique [39].

3.1. Thermal behavior during conventional heating and cooling scans in the DSC

Fig. 2 shows cooling traces corresponding to all the 80/20 blends (melt mixed and 'unmixed' blends) examined in this work as an example of how the dynamic crystallization was monitored in the DSC. A similar behavior was obtained for all the cooling scans from the melt, where upon cooling only one exotherm was present for the melt mixed blends and two very clear exotherms were encountered for the 'unmixed blends'. The cooling scans corresponding to the 'unmixed' blends was obtained by the weighted mathematical superposition of the corresponding neat components. Very similar traces can also be generated experimentally by placing the corresponding amount of each neat polymer separated by aluminum foil within the DSC pan (see Ref. [54]).

For the 'unmixed' 80/20 ULDPE/HDPE2, a relatively sharp crystallization peak corresponding to the HDPE2 component can be seen at approximately 115°C. Then, at lower temperatures, the bimodal wide crystallization range of the ULDPE can be observed. The higher temperature peak that appears at 77.5°C corresponds to the crystallization of the more linear fractions within ULDPE and this is followed at lower temperatures by a very broad exotherm where the shorter linear segments of fractions with higher branch contents can crystallize. When this DSC scan is compared to that of the melt mixed 80/20 ULDPE/HDPE2 blend, the fact that the most linear fractions within ULDPE had been nucleated is apparent since the 77.5°C peak has been shifted to higher temperatures and is now overlapped with the crystallization exotherm of the HDPE2 component. This nucleation process represents a significant increase (35.4°C) of the crystallization peak temperature in relation to neat ULDPE (whose crystallization behavior can be clearly observed in the lower temperature range of the

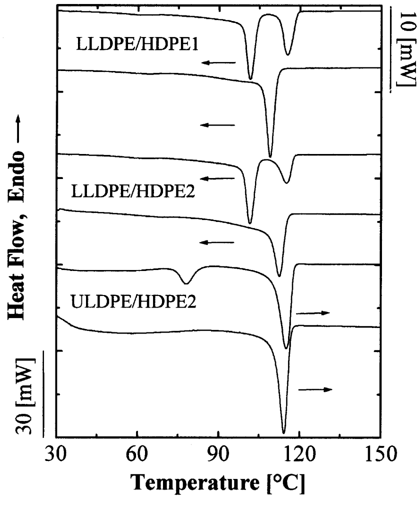

Fig. 2. DSC cooling scans from 170°C at 10°C/min, for the three types of blends at a fixed composition of 80/20 LLDPE/HDPE. For each blend system, the top DSC scan represents the 'unmixed' blend and the one below the melt mixed blend.

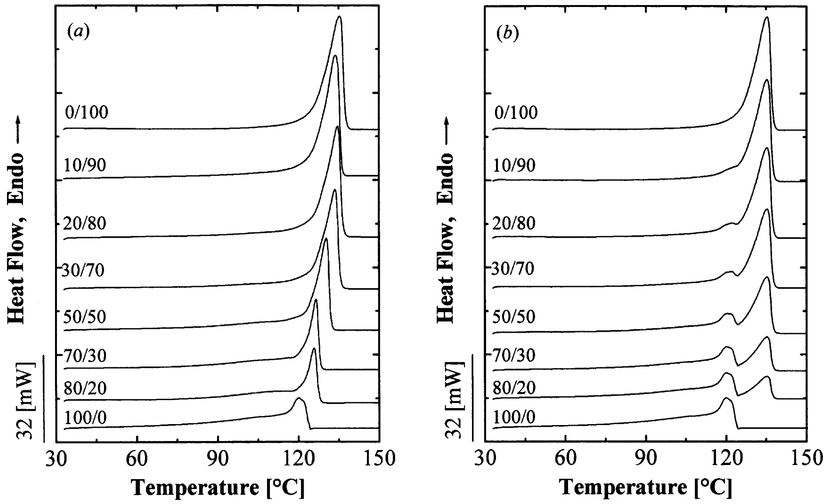

Fig. 3. DSC heating scans at 10°C/min for LLDPE/HDPE1: (a) melt mixed blends after cooling from 170°C at 10°C/min; (b) 'unmixed blends'.

80/20 'unmixed' ULDPE/HDPE2 blend), probably, due to the nucleation effect that the HDPE2 has over the more linear fractions of the ULDPE.

Fig. 2 also illustrates how an analogous nucleation process of LLDPE by HDPE1 or HDPE2 can be observed in the other two types of blends prepared here, namely LLDPE/HDPE1 and LLDPE/HDPE2. Further results on the cooling behavior of all systems studied in this work are reported in Fig. 4 and will be discussed below for each blend system examined here.

3.1.1. LLDPE/HDPE1 blends

Fig. 3a shows DSC heating curves for the LLDPE/HDPE1 blends after controlled cooling at 10°C/min. Only one melting endotherm is clearly observed for most compositions, a fact that may be considered as an indicator of partial miscibility [2,4,6–9], although not conclusively since the melting process could be influenced by a reorganization process during heating among other factors (see below).

However, careful observation of the melting traces, and above all in the blends that are rich in LLDPE, especially the 80/20, reveals that two melting signals are present. The one at high temperatures is very clear and sharp and could be attributed to the melting of co-crystals being formed by the HDPE1 chains together with the more linear fractions of the LLDPE. There is a broader second endotherm at lower temperatures which could correspond to the melting of the lamellae formed by the linear segments of the LLDPE chains with the highest SBC. However, as indicated below there may be an alternative explanation for these results.

Fig. 3b shows the melting behavior of the 'unmixed blends'. These traces were also generated in a mathematical way, as in the case of the cooling traces of Fig. 2, so they represent how the DSC melting scan would look if no interactions whatsoever between the components were present.

The 'unmixed blends' exhibit the expected superposition of the neat homopolymers thermal response in the DSC. Fig. 3b shows that most blend compositions exhibit two very clear melting endotherms, as opposed to the real melt mixed blends (Fig. 3a), which show only one endotherm. The differences are significant, above all, in the LLDPE/HDPE1 blends of composition 50/50, 70/30 and 80/20. One very important difference is that of the size of the endotherm corresponding to the LLDPE component. In the 'unmixed blends', the height and area of the LLDPE melting signal is proportional to its weight fraction in the blend (with respect to the latent heat of fusion of each material). Therefore, in the 80/20 LLDPE/HDPE1 'unmixed blend', the height of the LLDPE melting peak is larger than that of the HDPE1 peak in view of the large compositional variation.

Another important difference between Fig. 3a and b is the fact that the 30/70 and the 50/50 LLDPE/HDPE1 blend exhibit only one very clear melting endotherm at intermediate temperatures with respect to the melting peaks of the neat components while the corresponding 'unmixed blends' exhibit very clear double peaks. In other words, if there were absolutely no contact between the two neat polymers, the DSC would be able to differentiate the signals of the two components.

Fig. 4 shows that the peak crystallization (T_c) and melting (T_m) temperatures are dependent on the composition which could be a consequence of nucleation and/or co-crystallization processes. Fig. 4a shows the variations in T_c with composition and it is interesting to note that with only an addition of 10% of HDPE1 to the LLDPE, there was an increase in this temperature of 8.0°C. Such an increase in T_c could correspond to either a nucleation effect of the HDPE1 on the LLDPE or to a process of co-crystallization between the linear fractions of the LLDPE and the HDPE1. In this way, the crystallization and melting behavior and the compositional dependence of T_c and T_m in the blends

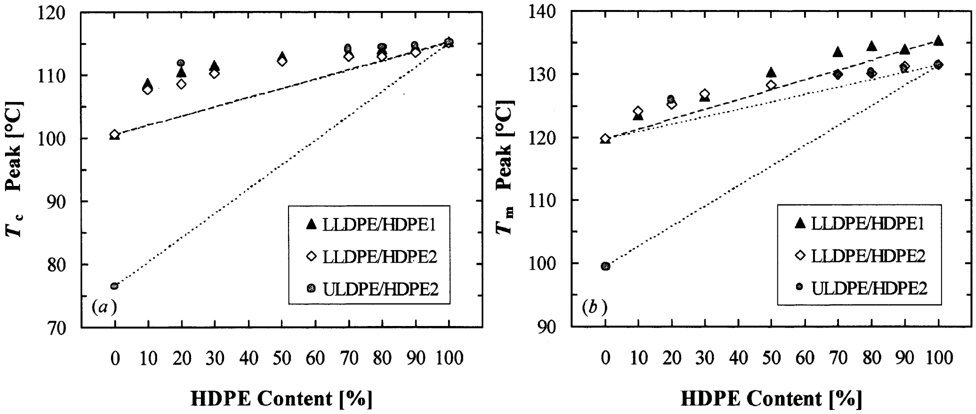

Fig. 4. Plots of (a) peak crystallization and (b) peak melting temperature as a function of blend composition.

(Fig. 4) could be explained in two possible ways:

(a) The formation of co-crystals during cooling from a partially miscible melt of LLDPE and HDPE1. In this case, the term partially miscible refers to the fact that the neat polymers are not immiscible and may form either one or two phases in the melt depending on the exact shape of their phase diagram [5].

(b) In the case that the blends are not miscible, the results may be due to a combined effect of:

- A nucleation phenomenon on LLDPE induced by HDPE1, a fact that would tend to increase both T_c and T_m of the LLDPE component (usually the shift in T_c would be higher than that of T_m).
- HDPE1 will crystallize in a melt of LLDPE chains and will melt also in the presence of molten LLDPE, this can induce a dilution effect that would certainly depress the melting point of the HDPE1 crystals, besides lowering T_c.

The increase in the melting peak temperature for LLDPE crystals and the depression in the melting peak temperature of the HDPE favors the overlap of the two melting signals into one single signal in the DSC scan.

The discrimination between the interpretations (a) and (b) above, that is to say, between partial miscibility with the formation of co-crystals versus the combined nucleation effect of HDPE1 and diluting action of LLDPE, or indeed, a combination of both interpretations, is made difficult based only on the dynamic thermal behavior registered by DSC. For this reason, other tests and/or experimental techniques are required in order to discriminate which of these effects prevails, and to this effect, the results of SSA offered a greater amount of evidence that favors interpretation (b) as will be discussed below.

3.1.2. LLDPE/HDPE2 blends

Fig. 5a shows heating DSC scans of melt mixed LLDPE/HDPE2 blends, after a controlled cooling at 10°C/min. The general behavior is similar to that observed in the case of the LLDPE/HDPE1 blends. In the LLDPE/HDPE2 system, the DSC scans of the 'unmixed' blends not shown here exhibit two melting peaks that are much closer to one

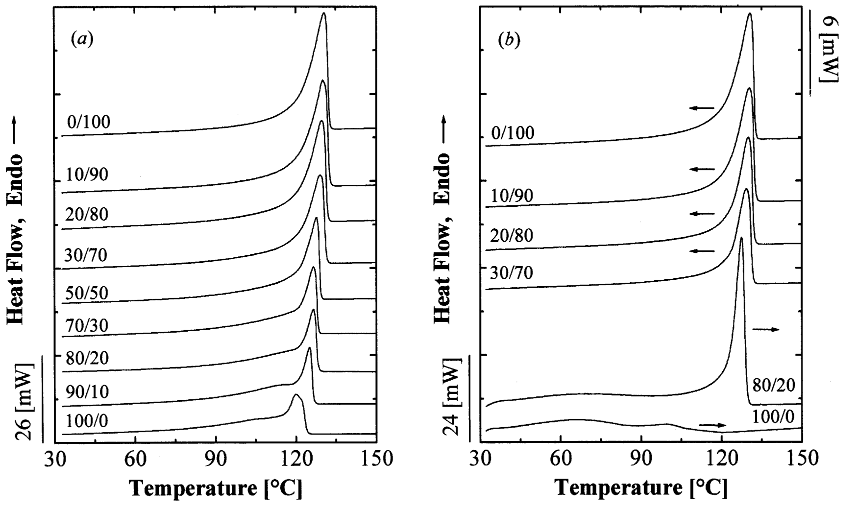

Fig. 5. DSC heating scans at 10°C/min for melt mixed blends after cooling from 170°C at 10°C/min: (a) LLDPE/HDPE2; (b) ULDPE/HDPE2.

another than in the case of the LLDPE/HDPE1 system, since HDPE2 is also an ethylene/1-butene copolymer.

It would require other experiments, such as isothermal crystallization or, as pointed out below, SSA, to discriminate between the effects of co-crystallization due to miscibility, or a combined effect of nucleation of LLDPE by the HDPE2 during crystallization, and the overlap of the melting signals of both types of PE favored by the dilution effect of the melted LLDPE over the crystals of HDPE2, as mentioned above for the LLDPE/HDPE1 blends.

3.1.3. ULDPE/HDPE2 blends

Fig. 5b shows heating DSC scans of ULDPE/HDPE2 blends, after a controlled cooling at 10°C/min blends. The melting behavior of neat ULDPE is also shown in Fig. 5b. This polymer starts melting at temperatures well below the starting temperature of this scan as is usually the case for a highly branched PE. In the temperature range explored in Fig. 5b, it exhibits a very wide melting range with two maxima located at 70 and 100°C, this corresponds to a very wide bimodal distribution of lamellar thickness originating from a heterogeneous distribution of comonomers.

Table 2 shows the marked differences between ULDPE and HDPE2 as regards to crystallization and melting temperatures. The melting behavior that is shown in Fig. 5b for the ULDPE/HDPE2 blends seems to be controlled, principally, by the characteristics of the HDPE2.

The DSC heating scans for the 'unmixed' ULDPE/HDPE2 blends (not shown here) reveal that in view of the great differences in enthalpy of fusion between both neat polymers and the broad melting range of HDPE2, the contribution of the ULDPE can hardly be appreciated in blend compositions with more than 50% HDPE2.

In the case of the 80/20 ULDPE/HDPE2 blend, Fig. 5b shows that the second melting signal corresponding to ULDPE component which was around 100°C has almost disappeared. The decrease in size of this signal could be due to an overlap in the tail end of the HDPE2 melting signal. On the other hand, the ULDPE component melting signal at 70°C in the 80/20 blend is wider corresponding to the melting of crystals formed by shorter linear sequences. In other words, if there were a nucleating effect of the HDPE2 over the ULDPE or partial miscibility, it would appear that only the more linear fractions of the latter were affected.

Fig. 4 shows a comparison of the trends in the variations of the peak crystallization and melting temperatures for all of the three systems evaluated in this work. Both crystallization and melting peaks appear to strongly depend on the behavior of the HDPE present in the blend.

In the case of the peak crystallization temperature, both neat HDPEs show the same crystallization temperature, thus the behavior for the three systems is similar in Fig. 4a. A slightly higher depression on the crystallization temperature of LLDPE/HDPE2 blends upon increasing LLDPE content can be appreciated in comparison with LLDPE/HDPE1 blends. This difference could be interpreted as a result of a greater miscibility between LLDPE and HDPE2, a fact that could cause co-crystallization between several fractions of both materials.

The melting peak temperatures shown in Fig. 4b appear to depend, fundamentally, on the HDPE used in the blends. It is important to point out that reorganization processes during the scan may also play a role here since even though the crystallization temperature of both HDPE1 and HDPE2 are the same, their melting temperature is different. This fact is probably linked to different reorganization rates for each HDPE during the scan in view of their distinct molecular composition (i.e. one is basically a homopolymer and the other a bimodal copolymer, see Table 1) [52,53].

The behavior shown for the melting temperature peaks of the LLDPE/HDPE2 and ULDPE/HDPE2 systems, in which the same HDPE is used, is very similar (in particular for the HDPE2 rich blends), which confirms that it is the type of HDPE that fundamentally governs the resulting peak melting temperatures for the blends.

3.2. Thermal behavior after SSA treatment

3.2.1. LLDPE/HDPE1 blends

Fig. 6a shows DSC heating scans of the LLDPE/HDPE1 blends after having been subjected to a six-step SSA treatment, with the following T_s temperatures for self-nucleation and/or annealing: 134, 129, 124, 119, 114 and 109°C (more details of the technique and its applications to several systems are reported in Refs. [39–42]).

The series of melting endotherms that can be observed in the DSC heating scans of Fig. 6a indicate that thermal fractionation has occurred during the SSA treatment. Each fusion endotherm, therefore, corresponds to the melting of a particular lamellar population made up of the linear sections of chains with similar SBC and distribution. The fractions that exhibit the highest melting points are those with the longest linear segments incorporated within that specific lamellar population and therefore they would be the ones with the lowest SBC [39–42].

The results of Fig. 6a indicate that neat homopolymer HDPE1 is very difficult to fractionate in view of its negligible branching content. Therefore, the limited impact the SSA treatment had on its melting point distribution is due to the poor ability of the technique to induce molecular weight fractionation with the short times applied at each T_s in this case. We also applied to this HDPE1 an SSA treatment using steps separated by a 2.5°C window instead of our standard 5°C; nevertheless, the fractionation quality did not improve.

As has been demonstrated previously [39–42], the SSA procedure fractionates the polymer mainly by its branch content with a minor influence of the molecular weight distribution, at least in the case of PEs [42,47]. The SSA protocol used in this work was designed to cause fractionation by the segregation of short chain branching during each

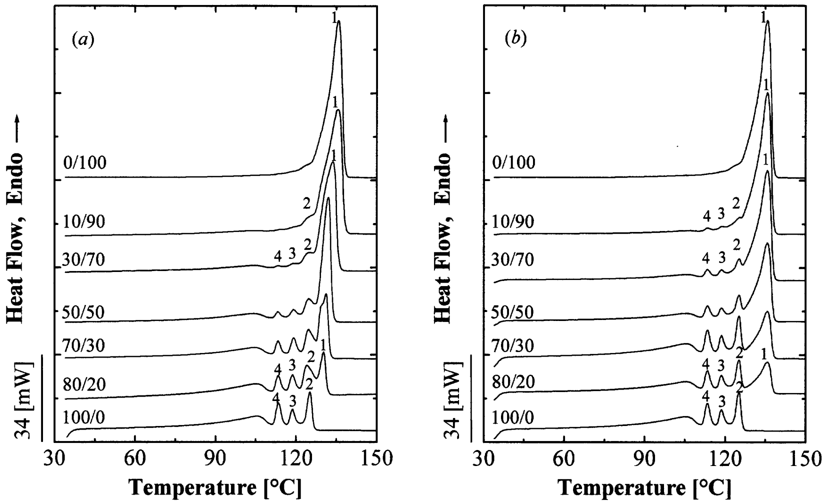

Fig. 6. DSC scans at 10°C/min after SSA treatment for LLDPE/HDPE1 blends: (a) melt mixed blends; (b) 'unmixed blends'.

step in the quickest and more efficient way [39–42]. The presence of a single signal in HDPE1 helps to indicate that the process of segregation by SSA is less sensitive to differences in molecular weight of the chains because the polydispersity of this material is close to 6 and still the fractionation was very limited.

It should be noted that in the case of other thermal fractionation techniques, such as TREF or stepwise crystallization, there is also no reported evidence of successful fractionation of materials with negligible branching content, at least with the usual fractionation times employed in these techniques [19,22,31,34]. In the case of TREF, it could be argued that the separation mechanism is somewhat different because the molecular fractionation is performed in solution and therefore the diffusion effects would be less restrictive. However, the mechanism behind other fractionation techniques in the bulk should be similar to SSA. Adisson et al. [22] report that after applying thermal fractionation to a polymer with a very low branching content no appreciable molecular segregation was obtained. Furthermore, Keating et al. [31] have applied thermal fractionation by SC methods to polymers with different polydispersities but similar SBC and obtained very similar qualities of fractionation.

The efficiency of the SSA treatment is revealed in the samples that possess chains with appreciable amounts of chain branching that can act as defects during crystallization and subsequent annealing. This is apparent in the heating scan shown in Fig. 6a of the neat LLDPE where four clear fractions were produced by the SSA treatment. The SSA method allows the observation of structural heterogeneity in the LLDPE since a separation of several fractions by SBC was made possible. A detailed analysis has been previously reported for the LLDPE used in this work using an extensive 14-step SSA, which revealed the bimodal nature of the distribution of the short branching and was in good agreement with an analysis of the same material performed by TREF [39].

The cooling DSC scans after each one of the isothermal steps of self-nucleation and/or annealing, exhibited shifts in the peak crystallization temperatures for the HDPE1 upon cooling from a T_s temperature of 129°C (not shown here), while in the LLDPE, the same phenomenon was observed upon cooling from 124°C [42]. These increments in the crystallization temperature are a consequence of the self-nucleation of the PEs at the indicated temperatures. A nucleation density increment of several orders of magnitude brings a reduction in the supercooling necessary for the crystallization. For LLDPE, this means that 124°C is a T_s temperature that causes only self-nucleation and that the first step of the SSA treatment that induces annealing is that when a T_s temperature of 119°C is used (see Table 3). Therefore, of the four fractions exhibited in the DSC heating scan of Fig. 6a for neat LLDPE, the highest melting three fractions correspond to those induced by the thermal fractionation steps of 119, 114 and 109°C, respectively (see Table 3). On the other hand, the lowest melting endotherm is the result of the fusion of the crystals formed during dynamic cooling at 10°C/min from the last T_s temperature applied, i.e. 109°C. Table 3 lists the peak melting temperatures of all the fractions produced by steps where annealing and self-nucleation took place at the indicated T_s temperatures.

In the case of the 80/20, 70/30, 50/50 and 30/70 LLDPE/HDPE1 melt mixed blends (Fig. 6a), the annealing of these samples occurred in the isothermal steps corresponding to T_s temperatures 124, 119, 114 and 109°C. For this reason in these blends, four sharp melting peaks (labeled 1–4 in Fig. 6a and Table 3) are shown in addition to the lowest melting temperature broad peak produced by the melting of the lamellae formed during the dynamic cooling before the melting scan shown in Fig. 6a. For the 10/90 LLDPE/HDPE1 blend, only one sharp melting peak (labeled 1 in Fig. 6a) and a low temperature shoulder (labeled 2) can be clearly observed since the proportion of LLDPE in the blend is small, and the behavior is dominated by HDPE1 which shows

Table 3
Melting temperature of blends evaluated by DSC after SSA treatment

HDPE content (%)	T_s (°C)			
	1: 124	2: 119	3: 114	4: 109
LLDPE/HDPE1				
0	–	125.2	118.7	113.5
20	130.4	124.2	118.7	113.4
30	131.2	124.7	119.2	113.4
50	132.0	124.7	119.2	113.2
70	135.7	125.0	119.3	113.2
90	135.7	124.7	119.5	–
100	135.9	–	–	–
LLDPE/HDPE2				
0	–	125.2	118.7	113.5
10	–	125.7	119.4	113.9
20	–	126.5	119.5	113.8
30	–	126.4	119.5	113.7
50	130.2	126.7	120.0	113.9
70	132.9	126.5	120.0	114.2
80	131.7	126.7	120.4	114.2
90	133.2	126.0	120.7	114.7
100	133.0	127.0	120.2	114.4
ULDPE/HDPE2				
0	–	–	120.5	115.0
20	129.5	127.0	120.0	114.5
70	131.9	127.2	120.5	115.4
80	131.2	126.7	120.0	114.7
90	131.5	126.9	120.2	114.9
100	132.2	127.1	120.3	114.9

regularity, that is to say, little capability for fractionation in view of its lack of defects or branching in the polymer chain.

Fig. 6b shows the expected behavior for LLDPE/HDPE1 blends after SSA, in the total absence of interactions between each component since they are the 'unmixed' blends theoretical scans (constructed from the weighted mathematical average of the DSC scans of the neat components). The main difference between the melt mixed and 'unmixed' blends is seen in the endotherm corresponding to the highest peak melting temperature (fraction 1 or peak 1) which, in the theoretical scans, remains at a constant temperature and therefore appears to be broader. In the case of the experimental behavior, a reduction of the peak melting temperature of the annealed fractions at 124°C (peak 1) with composition can be observed (see Table 3). These variations in peak melting temperatures, for the group of crystals annealed at 124°C, can be attributed to a dilution effect caused by the rest of the chains that are molten at that temperature (i.e. mainly LLDPE chains). Therefore, a depression of the melting point of these highly linear fractions is generated.

The variations of the melting peaks of all fractions with composition for melt mixed LLDPE/HDPE1 blends can be seen in Table 3. It is readily apparent how the temperature of fraction 1 (made up basically of HDPE1 chains) decreases as a result of an increase in the content of LLDPE in the blends. Also, it is evident that, for the rest of the groups of lamellae, the melting temperatures do not vary significantly with the composition of the blends (fractions 2–4). In general, the behavior of the melting point of the fractions with composition follows a simple rule of additivity.

Fig. 7 shows how the areas under each one of the endotherms of Fig. 6a varies with composition. These areas are related to the relative percentage of crystalline material that melts in each of the fractions present in Fig. 6a. They are calculated by integrating each peak between the relative minima that are next to them and they are expressed as a percentage with respect to the total melting enthalpy of the material in question (the 'partial areas' tools of Pyris™ 3.1 software of Perkin–Elmer was used to make the calculation). This is why for instance peak 1 of neat HDPE1 in Fig. 7 has a partial melting area of 85%, since the integration of peak 1 was made between the high temperature baseline (i.e. 145°C) and the change in slope present at the low temperature tail where a small second fraction is present (see Fig. 6a, curve 0/100 or neat HDPE1, where peak 1 is the highest melting endotherm). The mass of all tested samples, was standardized at 10 mg, allowing comparisons to be made between different samples.

The general behavior displayed in Fig. 7 can be described by a simple additive rule of mixing, where a linear dependence with blend composition is exhibited. Such behavior probably indicates that the miscibility of one material with the other is not significant. The results obtained can then be explained by a diluting effect of the LLDPE chains over the melting of the HDPE1 crystals and also by a nucleating effect of HDPE1 over the LLDPE during the controlled cooling, see Fig. 4.

The results of this section, therefore, show that at least after the SSA treatment (which promotes phase segregation during crystallization and annealing) the blended materials (LLDPE and HDPE1) do not exhibit clear signs of co-crystallization that may constitute an indirect evidence of melt miscibility before cooling.

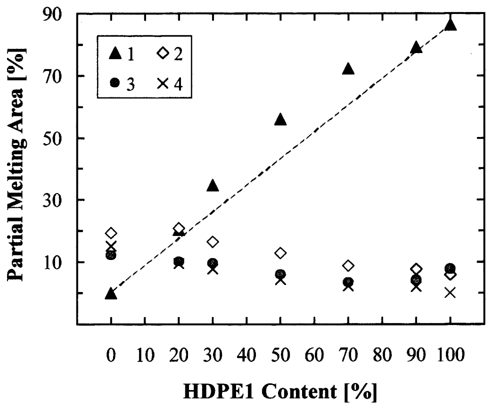

Fig. 7. Variation of partial melting areas with composition for LLDPE/HDPE1 blends after SSA treatment.

3.2.2. LLDPE/HDPE2 blends

The LLDPE/HDPE2 blends were subjected to the same SSA treatment as the LLDPE/HDPE1 systems. The melting behavior after SSA, shown in Fig. 8 for the LLDPE/HDPE2 system, presents important differences with regards to that of the LLDPE/HDPE1 blends.

Fig. 8a shows DSC melting scans after the SSA treatment was applied, using temperatures of 134, 129, 124, 119, 114 and 109°C. The neat HDPE2 shows four melting signals corresponding to groups of lamellae annealed at 124, 119, 114 and 109°C (see also Table 3). This material shows a larger number of segregated fractions than HDPE1 in view of its less regular backbone. HDPE2 is an ethylene/1-butene heterogeneous copolymer instead of a pure PE homopolymer like HDPE1, therefore, it can be fractionated using the SSA protocol applied in this work. Very similar copolymers have been evaluated in the literature by cross-fractionation procedures and the reported results indicate a complex dependence of fractionation quality on the molecular weight distribution and the short chain branching distribution [52].

In the case of the LLDPE/HDPE2 blends that are rich in HDPE2 (50/50, 30/70, 10/90), four melting signals are observed in Fig. 8a (labeled 1–4). The existence of these four endotherms was expected in view of the response of HDPE2 (the major component for these compositions) to the SSA treatment.

In the case of blends that are rich in LLDPE, i.e. 70/30, 80/20 and 90/10, as with neat LLDPE or 100/0, only three sharp melting signals can be seen in Fig. 8a. This is an unexpected result, since the blends do contain an appreciable amount of HDPE2 that should in theory respond to an annealing at 124°C (see also Table 3). In other words, it seems like the highest temperature fraction (i.e. fraction 1) that should be present is missing as can be clearly seen by comparing the theoretical scans of Fig. 8 with those of the real melt mixed blends in Fig. 8a for blend compositions 70/30, 80/20 and 90/10. In the case of the blends that are rich in HDPE2, a better molecular segregation and therefore thermal fractionation is obtained than in the blends that are rich in LLDPE.

The results shown in Fig. 8 can be interpreted as an indication that for blend compositions rich in LLDPE, co-crystals are formed between the chains of HDPE2 (in particular, those of fraction 1) and the more linear fractions of the LLDPE (i.e. fraction 2). The tendency to form these co-crystals and their stability must be high since SSA favors molecular segregation during crystallization. The behavior of partial miscibility for a range of compositions, has been reported by Norton and Keller [3], for an LLDPE/HDPE system, in experiments of isothermal crystallization after abrupt cooling from the melt.

As stated above, the comparison between Fig. 8a and b demonstrate the phenomena of partial miscibility in the LLDPE/HDPE2 blends. Four sharp maxima (fractions 1–4) are clearly seen in Fig. 8b for all the compositions in the 'unmixed' blends, contrary to the melt mixed blends of Fig. 8a, where the behavior of the blends rich in LLDPE differ from the expected and from the observed for the blends rich in HDPE2 (10/90, 20/80, 30/70 and 50/50). That is to say, there is a greater tendency of miscibility in the blends rich in LLDPE than in those rich in HDPE2.

Table 3 also lists the peak melting temperature of the fractions corresponding to the LLDPE/HDPE2 blends. In particular, there is evidence of a shift to lower temperatures in the peak melting temperatures corresponding to the group of lamellae annealed at 124°C (fraction 1), with composition (see Table 3). For the group of blends of compositions 50/50, 70/30, 80/20 and 90/10, the number of signals found experimentally is equal to the those found theoretically and approaches the expected behavior, in absence of miscibility between the components of the blend. This drop in peak melting temperatures with composition, for the fractions annealed at 124°C, could be a consequence of the

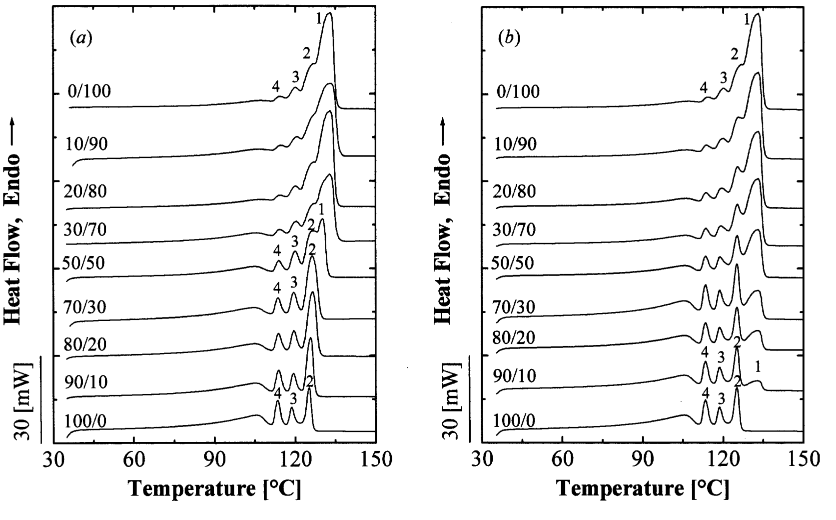

Fig. 8. DSC scans at 10°C/min after SSA treatment for LLDPE/HDPE2 blends: (a) melt mixed blends; (b) 'unmixed blends'.

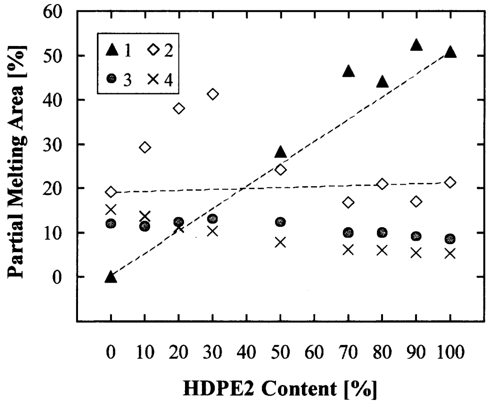

Fig. 9. Variation of partial melting areas with composition for LLDPE/HDPE2 blends after SSA treatment.

dilution effect of the melted chains of LLDPE over the melting of lamellae formed principally by macromolecules of HDPE2. In the same composition range, the other three fractions do not seem to shift their melting peaks with composition (see Table 3).

The behavior of the partial melted areas, in relation to the composition of the LLDPE/HDPE2 blends, is reported in Fig. 9. The results show that several fractions behaved according to the expectation of a simple rule of mixtures, like those of LLDPE/HDPE1. The fractions 1, 3 and 4 that correspond to groups of lamellae annealed at 124, 114 and 109°C (see also Table 3) exhibit a behavior close to linearity in those cases where the signal is present.

On the other hand, there is evidence in Fig. 9 of a marked positive deviation of the rule of mixing in the partial melted areas corresponding to the fraction annealed at 119°C for the blends that are rich in LLDPE. This positive deviation could be a consequence of the partial miscibility between LLDPE and HDPE2. The miscibility of these compositions rich in LLDPE leads to the formation of LLDPE and HDPE2 co-crystals that are annealed at 119°C. This also explains the absence of a melting signal and its respective partial area for groups of lamellae that should have been annealed at 124°C and that would have been formed, primarily, by HDPE2 chains in immiscible blends. In summary, for the blends that are rich in LLDPE, as a result of the co-crystallization, the partial melted areas corresponding to the melting of annealed crystals at 119°C (fraction 2) are much greater than expected in the absence of interactions.

Table 3 shows that the melting peak temperatures corresponding to the annealed crystals at 119°C for LLDPE/HDPE2 blends do not vary significantly with composition. This indicates that the lamellae corresponding to this fraction have similar thickness for all blend compositions and that the increase in the partial melted area of LLDPE rich blends is a consequence of the melting of a greater quantity of material due to co-crystallization between fractions of HDPE2 and of LLDPE. This co-crystallization of fractions 1 and 2 of LLDPE and of HDPE2 is possible since both materials are structurally similar (i.e. they are both Ziegler–Natta type ethylene/1-butene copolymers).

In a study of LLDPE/VLDPE blends, which are characterized by DSC using SC, Shanks and Amarasinge [50] also show differences in the experimental DSC scans of the blends after fractionation by SC and the theoretical scans and related these differences with processes of partial miscibility; nevertheless, a nucleating action of some LLDPE fraction on the VLDPE most linear fractions could also contribute to the effect observed. Fonseca and Harrison [49] characterized blends of LDPE/HDPE by TREF and DSC, and found that by implementing abrupt cooling, a fraction of co-crystals rich in LDPE is produced. The miscibility of the LLDPE/HDPE2 system presented in this work seems to be greater because, even after a treatment such as SSA that promotes segregation, there still is evidence of co-crystallization.

3.2.3. ULDPE/HDPE2 blends

Fig. 10a shows the final melting behavior of the ULDPE/HDPE2 system after SSA. This system was submitted to a 16-step SSA treatment with temperature intervals between 134 and 59°C (every 5°C). In the case of neat ULDPE, 12 sharp melting signals corresponding to 12 thermal fractions can be observed (the first four T_s temperatures used are wasted for neat ULDPE in view of the lower melting temperature as compared to HDPE2). Such behavior implies that neat ULDPE exhibits a great heterogeneity in its distribution of short chain branching including a small amount of linear rich fractions [39,40]. Indeed, for a complete fractionation of the material, a greater number of cycles with even lower T_s temperatures would be required, as indicated in Fig. 10 by the broad melting process, which is known to start at sub-room temperatures [52].

In the case of the HDPE2 and in all the blends, the process of annealing started at T_s temperatures of 124°C. In the case of neat HDPE2, T_s temperatures lower than approximately 100°C are not very effective in causing any fractionation (see Fig. 10a) since the quantity of material that melts at $T < 100$°C is very small.

The DSC heating scans of Fig. 10a, for blends rich in HDPE2 after the SSA treatment, show a behavior very similar to that found for neat HDPE2. The DSC scans corresponding to the melt mixed blends (Fig. 10a) are very similar to those of the 'unmixed' blends (Fig. 10b), in the case of blends that are rich in HDPE2 and this could indicate that the prevailing behavior is segregation.

For the 80/20 ULDPE/HDPE2 blend, a melting point depression for the fraction annealed at 124°C can be observed and is probably caused as in previous cases by a dilution effect of the rest of the molten material. Incidentally, this is the only composition for which a difference between the melt mixed and the 'unmixed' blends can be observed. As can be seen by comparing Fig. 10a and b, the size of the second sharp melting

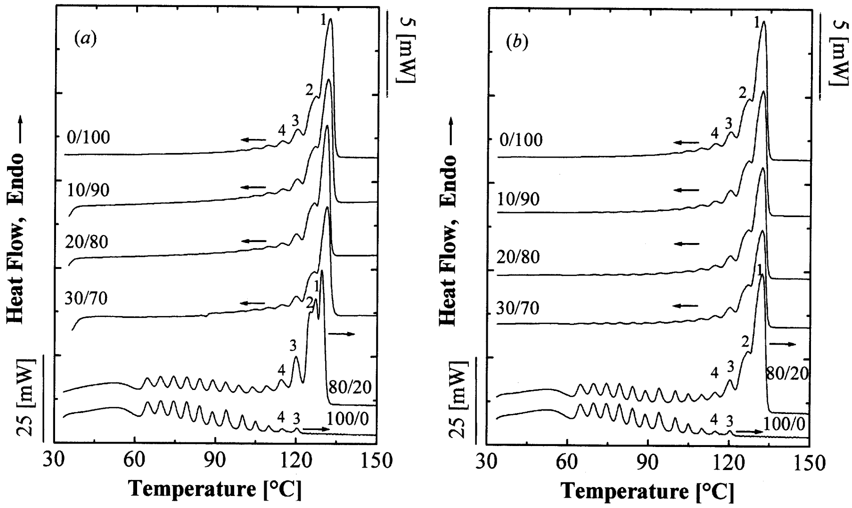

Fig. 10. DSC scans at 10°C/min after SSA treatment for ULDPE/HDPE2 blends: (a) melt mixed blends; (b) 'unmixed blends'.

fraction, whose maximum melting is found at 127°C (see also Table 3), is higher than in the theoretical blend. This result could be a consequence of some miscibility or co-crystallization process between a small proportion of similar short chain branched molecules of ULDPE (probably the most linear ones) and mainly HDPE2 chains.

The behavior of the partial melting areas as a function of composition for ULDPE/HDPE2 blends is shown in Fig. 11. It seems to follow a simple additive mixing rule for fractions 2–4 (those produced by annealing at T_s temperatures of 119, 114 and 109°C, see Table 3), which indicates that the segregation of the neat materials prevails. Only do the fractions annealed at 124°C (fraction 1 in Fig. 11 or Table 3) show a slight positive deviation from simple additivity of their partial melting area vs. composition trend. The peak melting temperatures for the fractions are all constant with composition as indicated in Table 3 except for the already mentioned exception of fraction 1, where a dilution effect was observed.

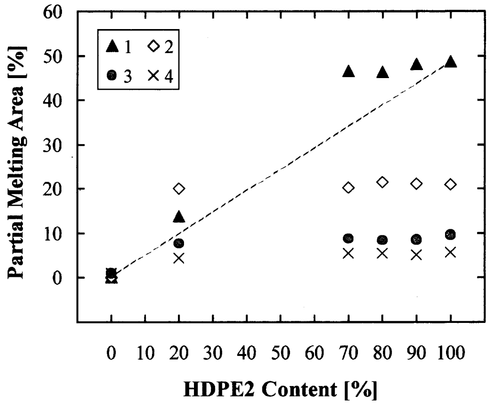

Fig. 11. Variation of partial melting areas with composition for ULDPE/HDPE2 blends after SSA treatment.

3.3. Comparative analysis of the results for the three blend systems

It is interesting to compare the observed behavior presented above for all three blend systems. The trend found upon evaluating only the crystallization and melting process in a dynamic way (Figs. 2–5), is basically the same for all blends, with minor differences in the variation of the crystallization and melting temperatures with composition and the shape of the endotherm tail that is extended to lower temperatures. However, after the SSA treatment one can observe significant differences in the systems examined.

For all the blends studied here, the interpretation of dynamic cooling and heating in the DSC indicate that the following effects are produced:

(a) A nucleating effect of the HDPE on LLDPE or ULDPE crystals.
(b) A slight increase in the melting temperature of the crystals formed by the most linear fractions of LLDPE, as a consequence of the increase in crystallization temperature caused by the nucleation effect mentioned in (a).
(c) A dilution effect caused by the less regular material in the liquid state (i.e. molten LLDPE or ULDPE) over the melting points of the lamellae formed by the more regular chains coming from the HDPE (a melting point depression effect similar to that caused by a solvent).
(d) Reorganization processes during the heating scans that may lead to annealed crystals with higher melting points.
(e) To a much lesser degree, there could also be some partial miscibility between certain fractions in both components.

However, after applying the SSA treatment to the LLDPE/HDPE1 and ULDPE/HDPE2 blends, what predominates is the molecular segregation of both materials without any significant miscibility. The nucleation, dilution and reorganization effects mentioned above also remained present for some of the fractions produced. The results indicate that simple additivity of blend components is followed, and linear tendencies for the evolution of the partial melted areas and melting peak temperatures of the fractions are observed.

In the case of the LLDPE/HDPE2 blends, after treatment with SSA, interesting effects were produced. Mainly, the number of thermal fractions generated by SSA in the blends varied with composition, a fact that is explained by processes of partial miscibility between chains of specific SBC of each copolymer for blend compositions rich in LLDPE.

The SSA treatment fundamentally promotes molecular segregation. Therefore, even under conditions that are appropriate for the segregation of the blend components, in the LLDPE/HDPE2 system, there exists miscible fractions in the melt with a capacity to co-crystallize during cooling and subsequent SSA steps, as opposed to the LDPE1/HDPE1 system, where segregation prevails. This comparison stresses the capability of the SSA technique for the study of segregation and partial miscibility phenomena in PE blends, in a comparative way.

4. Conclusions

The application of the technique of SSA to the study of PE blends is useful as a quick and precise tool for making comparisons and ascertain miscibility between different types of PE blends.

As opposed to simple cooling and heating runs in the DSC where valuable but limited information on blend miscibility can be gathered, the results after SSA can differentiate blends that tend to phase segregate during cooling from those that can form stable co-crystals even after a thermal fractionation procedure that promotes molecular segregation by SBC.

The effects of nucleation and melting point depression, caused by one type of PE on the other when PEs of different branching contents are mixed, tend to produce an overlap of the crystallization and melting endotherms of conventional DSC cooling and heating scans that may lead to interpretations of partial miscibility. However, after SSA, even when the nucleation, reorganization during the heating scan and dilution effects are still present for some of the fractions produced, the thermal fractionation procedure helps to distinguish them from co-crystallization effects mainly by observing how the number of thermal fractions generated by SSA in the blends varies with composition and by comparing the relative amounts of the thermal fractions produced by SSA.

The results indicate that only those PE fractions that are similar in chemical structure, as regards to content and distribution of short chain branches, are probably miscible in the melt and can oppose molecular segregation during SSA and therefore produce stable co-crystals.

Acknowledgements

This work was made possible by the generous funding of the Consejo Nacional de Investigaciones Científicas y Tecnológicas from Venezuela, CONICIT, through grant G97-000594.

References

[1] Hamid SH, Atiqullah M. J Macromol Sci, Rev Macromol Chem Phys 1995;C35(3):495–515.

[2] Datta NK, Birley AW. Plast Rubber Process Appl 1982;2(3):237–45.

[3] Norton DR, Keller A. J Mater Sci 1984;19(2):447–56.

[4] Hu S, Kyu T, Stein RS. J Polym Sci, Polym Phys Ed 1987;25(1):71–87.

[5] Barham PJ, Hill MJ, Keller A, Rosney CCA. J Mater Sci Lett 1988;7(12):1271–5.

[6] Pracella M, Benedetti E, Galleschi F. Thermochim Acta 1990;162(1):163–77.

[7] Conde MT, Gedde UW. Polymer 1992;33(15):3123–36.

[8] Gupta AK, Rana SK, Deopura BL. J Appl Polym Sci 1992;44(4):719–26.

[9] Hay J, Zhou X. Polymer 1993;34(5):2282–8.

[10] Tashiro K. Acta Polym 1995;46(2):100–13.

[11] Wignall GD, Londono JD, Lin JS, Alamo RG, Galante MJ, Mandelkern L. Macromolecules 1995;28(9):3156–67.

[12] Schipp C, Hill MJ, Barham PJ, Cloke VM, Higgins JS, Oiarzabal L. Polymer 1996;37(12):2291–7.

[13] Kim BK, Kim KJ, Park SJ, Jeong HM. J Polym Engng 1992;11(4):297–314.

[14] Vogl O. J Macromol Sci, Pure Appl Chem 1998;A35(7–8):1017–35.

[15] Bruni C, Pracella M, Masi F, Menconi F, Ciardelli F. Polym Int 1994;33(3):279–84.

[16] Mathot VBF, Scherrenberg RL, Pijpers MPJ, Bras W. J Therm Anal 1996;46(3–4):681–718.

[17] Popli R, Mandelkern L. J Polym Sci, Polym Phys Ed 1987;25(3):441–83.

[18] Starck P. Polym Int 1996;40(2):111–22.

[19] Wild L, Ryle TR, Knobeloch DC, Peat IR. J Polym Sci, Polym Phys Ed 1982;20(3):441–55.

[20] Monrabal B. J Appl Polym Sci 1994;52(4):491–9.

[21] Schouterden P, Groeninckx G, Van der Heijden B, Jansen F. Polymer 1987;28(12):2099–104.

[22] Adisson E, Ribeiro M, Deffieux A, Fontanille M. Polymer 1992;33(20):4337–42.

[23] Kamiya T, Ishikawa N, Kambe S, Ikegami N, Nishibu H, Hattori T. In: Proceedings of SPE-ANTEC, 1990; TX, USA. p. 871–3.

[24] Liu TM, Harrison IR. Thermochim Acta 1994;233(1):167–71.

[25] Keating MY, McCord EF. Thermochim Acta 1994;243(2):129–45.

[26] Mara JJ, Menard KP. Acta Polym 1994;45(5):378–80.

[27] Balbontin G, Camurati I, DallÓcco T, Finotti A, Franzese R, Vecellio G. Angew Makromol Chem 1994;219:139–60.

[28] Chiu FC, Keating MY, Cheng SZD. In: Proceedings of SPE-ANTEC, 1995; MA, USA. p. 1502–5.

[29] Minick J, Moet A, Hiltner A, Baer E, Chum SP. J Appl Polym Sci 1995;58(8):1371–84.

[30] Wolf B, Kening S, Klopstock J, Miltz J. J Appl Polym Sci 1996;62(9):1339–45.

[31] Keating M, Lee IH, Wong CS. Thermochim Acta 1996;284(1):47–56.

[32] Lehtinen C, Starck P, Löfgren B. J Polym Sci, Part A: Polym Chem 1997;35(2):307–18.
[33] Zhang M, Huang J, Lynch DT, Wanke S. In: Proceedings of SPE-ANTEC, 1998; GA, USA. p. 2000–3.
[34] Shanks RA, Drummond K. In: Proceedings of SPE-ANTEC, 1998; GA, USA. p. 2004–6.
[35] Liu W, Kim S, Lopez J, Hsiao B, Keating MY, Lee LH, Landes B, Stein RS. J Therm Anal Cal 2000;59(1–2):245–55.
[36] Shanks RA, Amarasinghe G. J Therm Anal Cal 2000;59(1–2):471–82.
[37] Zhang MQ, Lynch DT, Wanke SE. J Appl Polym Sci 2000;75(7):960–7.
[38] Zhang MQ, Lynch DT, Wanke SE. Polymer 2001;42(7):3067–75.
[39] Müller AJ, Hernández ZH, Arnal ML, Sánchez JJ. Polym Bull 1997;39(4):465–72.
[40] Arnal ML, Hernández ZH, Matos M, Sánchez JJ, Méndez G, Sánchez A, Müller AJ. In: Proceedings of SPE-ANTEC, 1998; GA, USA. p. 2007–10.
[41] Arnal ML, Sánchez JJ, Müller AJ. In: Proceedings of SPE-ANTEC, 1999; NY, USA. p. 2329–33.
[42] Arnal ML, Balsamo V, Ronca G, Sánchez A, Müller AJ, Cañizales E, Urbina de Navarro C. J Therm Anal Cal 2000;59(1–2):451–70.
[43] Gray AP, Casey K. J Polym Sci, Polym Lett 1964;2(4):381–8.
[44] Fillon B, Wittman JC, Lotz B, Thierry A. J Polym Sci, Part B: Polym Phys 1993;31(10):1383–93.
[45] Márquez L, Rivero I, Müller AJ. Macromol Chem Phys 1999;200(2):330–7.
[46] Balsamo V, Müller AJ, Stadler R. Macromolecules 1998;31(22):7756–63.
[47] Sabino M, Feijoo JL, Müller AJ. Polym Degrad Stab 2000, submitted for publication.
[48] Joskowicz PL, Muñoz A, Barrera J, Müller AJ. Macromol Chem Phys 1995;196(1):385–98.
[49] Fonseca CA, Harrison IR. Thermochim Acta 1998;313(1):37–41.
[50] Shanks RA, Amarasinghe G. Polymer 2000;41(12):4579–87.
[51] Wunderlich B. Thermal analysis. London: Academic Press, 1990 (Appendix).
[52] Mathot VBF. The crystallization and melting region. In: Mathot VBF, editor. Calorimetry and thermal analysis of polymers. Munich: Carl Hanser, 1994. p. 231–99.
[53] Puig CC, Avilés MV, Joskowicz P, Díaz A. J Appl Polym Sci 2001;79(11):2022–8.
[54] Müller AJ, Balsamo V. Thermal characterization in low density and linear low density polyethylene blends. In: Kohudic MA, editor. Advanced in polymer blends and alloys technology, vol. 5. Lancaster: Technomic Publishing, 1994. p. 1–21.